CSIRO PUBLISHING

Australian Journal of Physics

Volume 50, 1997

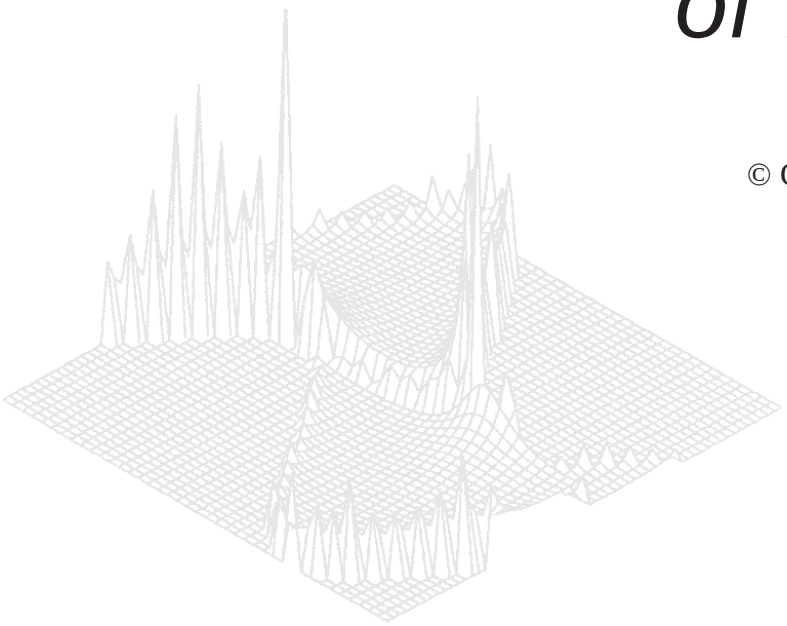

A journal for the publication of
original research in all branches of physics

www.publish.csiro.au/journals/ajp

All enquiries and manuscripts should be directed to
Australian Journal of Physics
CSIRO PUBLISHING
PO Box 1139 (150 Oxford St)
Collingwood Telephone: 61 3 9662 7626
Vic. 3066 Facsimile: 61 3 9662 7611
Australia Email: peter.robertson@publish.csiro.au

Published by **CSIRO** PUBLISHING
for CSIRO Australia and
the Australian Academy of Science

Aust. J. Phys., 1997, **50**, 759–71

Physical Processes determining the Antarctic Sea Ice Environment*

Ian Allison

Antarctic CRC and Australian Antarctic Division,
GPO Box 252-80, Hobart, Tas. 7001, Australia.

Abstract

The Antarctic sea ice zone undergoes one of the greatest seasonal surface changes on Earth, with an annual change in extent of around 15×10^6 km^2. This ice, and its associated snow cover, plays a number of important roles in the ocean–atmosphere climate system: the high albedo ice cover restricts surface absorption of solar radiation and acts as a barrier to the exchange of mass and energy between the ocean and atmosphere, and salt rejected by the growing ice cover affects the ocean structure and circulation. Additionally, a number of sea ice feedback processes have the potential to play an important role in climate change.

The extent to which a sea ice cover modifies ocean–atmosphere interaction is primarily determined by the thickness and concentration of the ice, but these themselves are determined by ocean and atmospheric interaction. The thickness distribution of the pack is determined by both thermodynamic and dynamic processes: most important at the geophysical scale are the dynamic processes of ice drift and deformation, and of lead formation. Compared to the ice cover in the central Arctic Basin, the Antarctic sea ice is highly mobile. Drifting buoy studies show that the Antarctic pack can move at speeds of up to 60 km per day or greater, and that around most of the Antarctic coast, the drift of the pack ice is generally divergent, with divergence rates of 10% or more per day being observed under some circumstances. Consequently there is generally some open water within the Antarctic pack and much of the total ice mass forms by rapid growth within these areas. This influences the crystal structure of the ice and results in a considerable portion of the Antarctic pack (up to 25% in spring-time) having a thickness of less than 0·3 m. In general much of the Antarctic sea ice only grows thermodynamically to about 0·5 m thick, with thickness increases beyond that resulting from the deformational processes of rafting and ridge-building.

1. Introduction

Each winter the surface water of a large area of the Southern Ocean freezes, forming a sea ice cover which greatly reduces the exchange of heat, gas and momentum between the ocean and atmosphere. This Antarctic sea ice zone undergoes an annual change in area from a minimum of about 4×10^6 km^2 to a maximum of 19×10^6 km^2 (about three times the area of Australia), one of the greatest seasonal surface changes on Earth. The ice, and its associated snow cover, play a number of important roles in the ocean–atmosphere climate system. It has a high albedo compared to that of open water and significantly reduces

* Refereed paper based on a plenary lecture given at the 12th Australian Institute of Physics Congress, held at the University of Tasmania, Hobart, in July 1996.

10.1071/PH96113 0004-9506/97/040759$05.00

the absorption of solar radiation at the surface. And the sea ice cover is also a very effective insulator, greatly restricting the loss of heat from the relatively warm ocean to the much colder atmosphere: during winter the turbulent heat loss from open water leads can be up to two orders of magnitude greater than from ice-covered ocean. The ice also influences ocean structure and circulation since, during ice formation and growth, salt is rejected to the underlying ocean, increasing the density of the water and setting up deep convection that contributes to the overall thermohaline circulation of the global ocean, and which can play a role in bottom water formation. When the ice subsequently melts it stabilises the upper ocean, and since ice formation and melt occur at in different regions, the equator-ward transport of ice results in a net northward flux of freshwater and negative heat.

The ocean, ice and atmosphere are part of a complex interactive system. While the ice influences the ocean and atmosphere, the distribution and characteristics of the ice are themselves forced by atmospheric and oceanic variables such as temperature, wind and salinity. Several of the resultant feedback processes have the potential to play an important role in global climate change.

Good data on Antarctic sea ice extent, and somewhat less accurate information on the ice concentration (that fraction of the ocean covered by ice), have now been available for nearly quarter of a century from passive microwave sensors on polar-orbiting satellites (Zwally *et al*. 1983; Gloersen *et al*. 1992). These data, however, show no statistically significant decrease in the ice extent (Gloersen and Campbell 1988; Johannesen *et al.* 1995) as might be expected from the results of global climate models for a period of recorded atmospheric temperature increase. However, significant interannual variations in the spatial distribution of the ice extent around the hemisphere have been observed at a periodicity of 4–5 years, and these are coupled to anomalies in the distribution of atmospheric pressure, wind stress and temperature in the Southern Ocean (White and Peterson 1996).

The satellite passive microwave data are of coarse resolution (25 km and greater) and provide little or no information on many important ice characteristics, especially ice thickness. The ice edge location is determined by advection as well as *in-situ* freezing, and changes in the total ice volume, for example, could occur without significant change to the ice edge, or to the mean ice concentration monitored by the satellite data. Only in the last decade or so, with the introduction of ice-breaking research vessels into service with a number of national Antarctic research programs, have climate scientists begun to build a total picture of the physical characteristics of the ice and of the major processes occurring within the sea ice zone during winter.

This paper is a review of some of the recent studies, with an emphasis on Australian investigations off the coast of East Antarctica.

2. General Ice Characteristics in the Antarctic Sea Ice Zone

In contrast to the conditions during summer when the remnant pack consists of floes of generally uniform appearance and of thickness greater than $0{\cdot}6$ m, the winter and spring-time pack in the Antarctic is a diverse mix of ice of different thickness categories and open water in leads (Jacka *et al*. 1987; Wadhams *et al*. 1987; Allison *et al*. 1993). In mid to late spring, as much as 30% of the total area of some parts of the Indian Ocean sector of the Antarctic Ocean may consist

of new ice less than 0·3 m thick with no or very little snow cover, and with up to a further 30% open water (Allison and Worby 1994). In winter and early spring there is less open water, but still a substantial fraction of new, thin ice.

At the outer ice edge during the growth season, active ice formation occurs by nucleation of small crystals (frazil) within the upper water column. These ice crystals are herded by wind and wave action into agglomerations that eventually consolidate into roughly circular pieces of new ice with upturned edges, known as pancake ice. The pancakes grow into larger sheets and thicken by bonding together and by rafting on top of each other, leaving areas between them which are relatively free of crystals and which act as source areas for new crystals (Lange *et al.* 1989). Further within the ice edge the frazil which forms in relatively protected areas within leads consolidates into continuous new flexible sheets, called nilas, 0·1 m to 0·2 m thick. These sheets buckle easily at the slightest disturbance, easily rafting to form thicker floes and creating new open water areas.

Although new ice forms most rapidly in open water areas, ice accretion also occurs on the bottom of existing floes as a result of heat removal from the ice–water interface by conduction through the floe. In contrast to the small randomly oriented grains of ice that form from aggregation of frazil, congelation ice growing on the underside of existing floes consists of characteristic long columnar crystals, with horizontal c-axes. New ice can also be formed when the snow cover on a floe is sufficiently heavy to depress the ice surface below sea level, saturating the near-surface snow with sea water and refreezing as 'snow-ice'. Because ice is such an effective insulator, this is a much more efficient method of ice growth than bottom freezing. Texturally this ice is similar to that formed from coarse grained frazil. However, compared to sea water, Antarctic snow is relatively depleted in the ratio of the heavy stable isotope of oxygen, ^{18}O, to that of ^{16}O, and ice that has formed by this process can be discriminated from frazil by isotope ratio measurements. Snow-ice will, however, have a stable isotope ratio that varies with the relative mix of meteoric water and seawater in the ice.

As well as influencing the mechanical, thermal and electrical properties of the material, the ice texture also provides information on the relative importance of different formation processes (Lange 1988). Gow *et al.* (1982) were among the first to show the large fraction of frazil in Weddell Sea ice, and hence the relative importance of rapid ice growth in open water areas. Similar results have since been found in many other parts of the Antarctic pack (e.g. Jeffries and Weeks 1993; Allison and Worby 1994). Fig. 1 shows typical textural, salinity and $\delta^{18}O$ profiles for a number of cores taken from floes in the Indian Ocean sector. In these, rafted floes can be identified by repeated layers of frazil and congelation crystals or by multiple 'c-curves' in the salinity profile. The profiles show that much of the ice >0·3 m thick has been rafted or ridged, and suggest that the increases in ice thickness beyond 0·4–0·5 m are usually the result of these dynamic processes. Worby *et al.* (1997) examined more than 150 cores collected between 60°E and 140°E, with an average length of 0·66 m, to determine that in this region 48% of the total ice mass forms by rapid freezing in open water, 39% by accretion on existing floes, and 13% by the freezing of sea-water saturated snow. Other areas around the Antarctic show a similar apportioning of ice formation. In the Weddell Sea, Lange and Eicken (1991) report 43% columnar ice and 16% snow

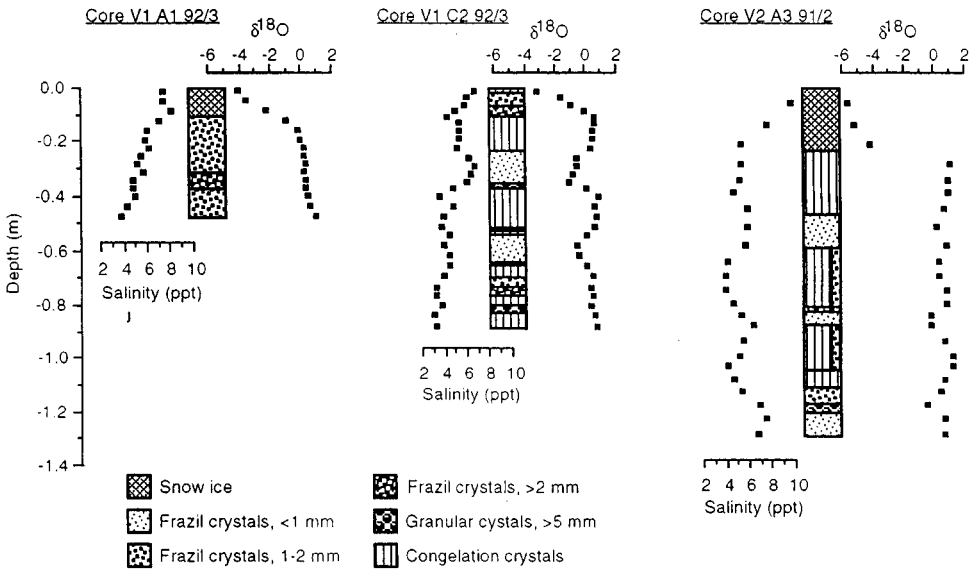

Fig. 1. Salinity, textural and δ^{18}O profiles from vertical ice cores sampled from typical ice floes in the east Antarctic sea ice zone. Salinity and δ^{18}O were measured on 2 to 5 cm horizontal sections of core, and crystal texture was examined in vertical thick sections. The cores show the difference between long columnar crystals of congelation ice that has accreted on the underside of existing floes, granular frazil ice resulting from rapid ice formation in open water, and granular snow-ice with negative δ^{18}O values.

ice, while in the generally thicker pack in the Bellingshausen and Amundsen Seas (60°W–135°W) Jeffries *et al.* (1997) report a snow-ice fraction as high as 25%.

The salinity of sea ice is considerably lower than that of sea water. Surface sea water around the coast of East Antarctica typically has a salinity between 33·5% and 34·0%, while ice cores sampled in the same region averaged 3·9% (Worby *et al.* 1997). The average salinity generally decreases with increasing ice thickness since the ice continues to desalinate with age, and to provide a salt flux to the ocean over a period of time, not just during the initial growth phase. The salinity variation with thickness in Antarctic ice is similar to that in Arctic sea ice, despite structural differences.

The size of individual pieces of pack ice, the floes, varies markedly with location and with time. Floes continuously change in size and shape, with one of the main mechanisms affecting their size being the penetration of swell into the pack. Long wave swell generated by storms in the Southern Ocean can penetrate hundreds of kilometres into the pack and break large floes into smaller rectilinear pieces. These become more rounded with time as they move and collide, creating broken brash ice between the floes. Floe break-up by swell effectively creates small areas of open water and enhances the ocean–atmosphere heat flux.

3. Ice and Snow Thickness

The thickness of sea ice, and of the snow cover on it, controls the surface albedo and the insulating effect of the pack, and hence determines the ocean–atmosphere

interaction. Energy exchange by turbulent transfer and radiation from areas of snow-free thin ice and open water dominate the total surface heat budget within the sea ice zone.

Until relatively recently, however, there were few systematic data on the thickness of ice and snow on the Southern Ocean. Wadhams *et al.* (1987) reported an average thickness of un-ridged ice floes in the eastern Weddell Sea, based on drilled measurements and ship-based observations, of only $\sim 0 \cdot 3$ m at the ice edge, increasing to $\sim 0 \cdot 6$ m close to the coast. In the Indian Ocean sector, Jacka *et al.* (1987) and Allison (1989) showed that the pack ice during late spring, near or soon after the maximum ice extent, was comprised of a broad mixture of ice types, thicknesses and floe sizes, with a total ice concentration generally higher than 80%, but with a high fraction (up to 25%) of ice thinner than $0 \cdot 3$ m. Allison *et al.* (1993), and subsequent cruises in the same area, give an average thickness of the un-ridged ice (averaged over the total area, including open water) in the Indian Ocean sector of only $0 \cdot 3$–$0 \cdot 4$ m, with an increasing ice thickness with distance south from the ice edge. Recent work in the Bellingshausen and Amundsen Seas (Worby *et al.* 1996*b*) shows that the ice there is only slightly thicker, with an area-weighted average of $0 \cdot 45$–$0 \cdot 5$ m.

Hourly ship-based observations have been collected on 18 Australian voyages to East Antarctica between October 1986 and August 1995 in order to determine the regional and seasonal variation in the ice and snow thickness distributions. The distribution of observations from these voyages, which cover all months of the year except for the winter period between May and June, is shown in Fig. 2. Each observation includes the ice thickness, snow thickness, floe size, extent of ridging, and partial concentration of up to three different ice categories around the vessel. Thus, the distribution of ice thickness and open water within the pack is recorded, as well as the mean thickness at each observation point.

Fig. 3*a* shows the derived ice and snow thickness distributions for a voyage in August 1995. This ice thickness distribution is typical for late-winter to early-spring, with a modal ice thickness between $0 \cdot 5$ and $0 \cdot 6$ m. A second peak of very thin ice occurs because of rapid ice formation in new leads as soon as they open. This thin ice increases quickly in thickness by both rafting and thermodynamic growth to $0 \cdot 5$–$0 \cdot 6$ m, but further growth beyond this is inhibited by the resistance of thicker floes to rafting over each other, and by the replacement of heat lost by conduction through the ice with heat from the ocean. This heat through the bottom of the near-surface mixed layer of the ocean from the deep ocean, the oceanic heat flux, reaches much higher values in the Antarctic than the Arctic because of the weaker vertical density gradients, and in many areas it limits thermodynamic ice growth. On the continental shelf near Mawson station the oceanic heat flux shows a strong seasonal variability and an annual average of between 5 and 12 $\mathrm{W\,m^{-2}}$ (Heil *et al.* 1996), and in the deeper ocean, values of 15 $\mathrm{W\,m^{-2}}$ are not uncommon (e.g. Worby *et al.* 1996*a*); a heat flux of 15 $\mathrm{W\,m^{-2}}$ is sufficient to melt $0 \cdot 5$ cm of ice per day.

Seasonally there are systematic changes in the ice thickness distribution averaged over the total ice area, with the greatest intra-annual changes occurring in the open water and thin ice categories. In March, at the beginning of the growth season, there is approximately 25% open water plus 60% newly formed ice less than $0 \cdot 4$ m thick. By August the open water fraction has decreased to 12% and

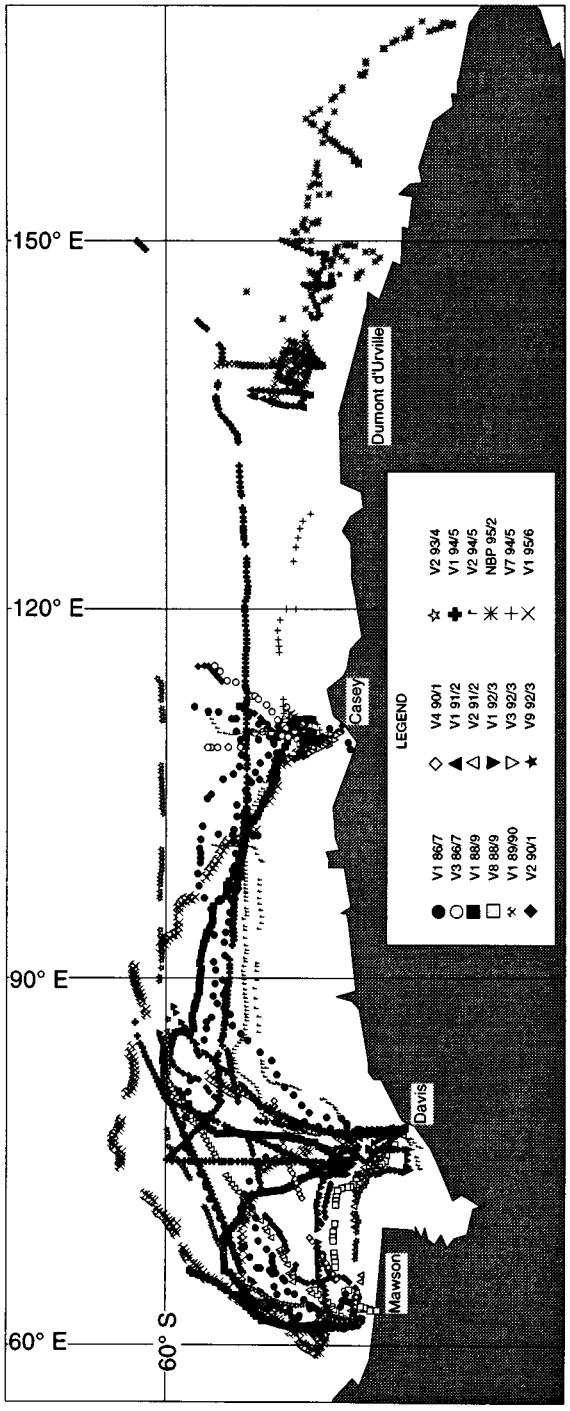

Fig. 2. Region of the Antarctic sea ice zone covered by Australian ship-based observations of ice characteristics and thickness. Symbols indicate samples and measurements on different cruises and at different times of year.

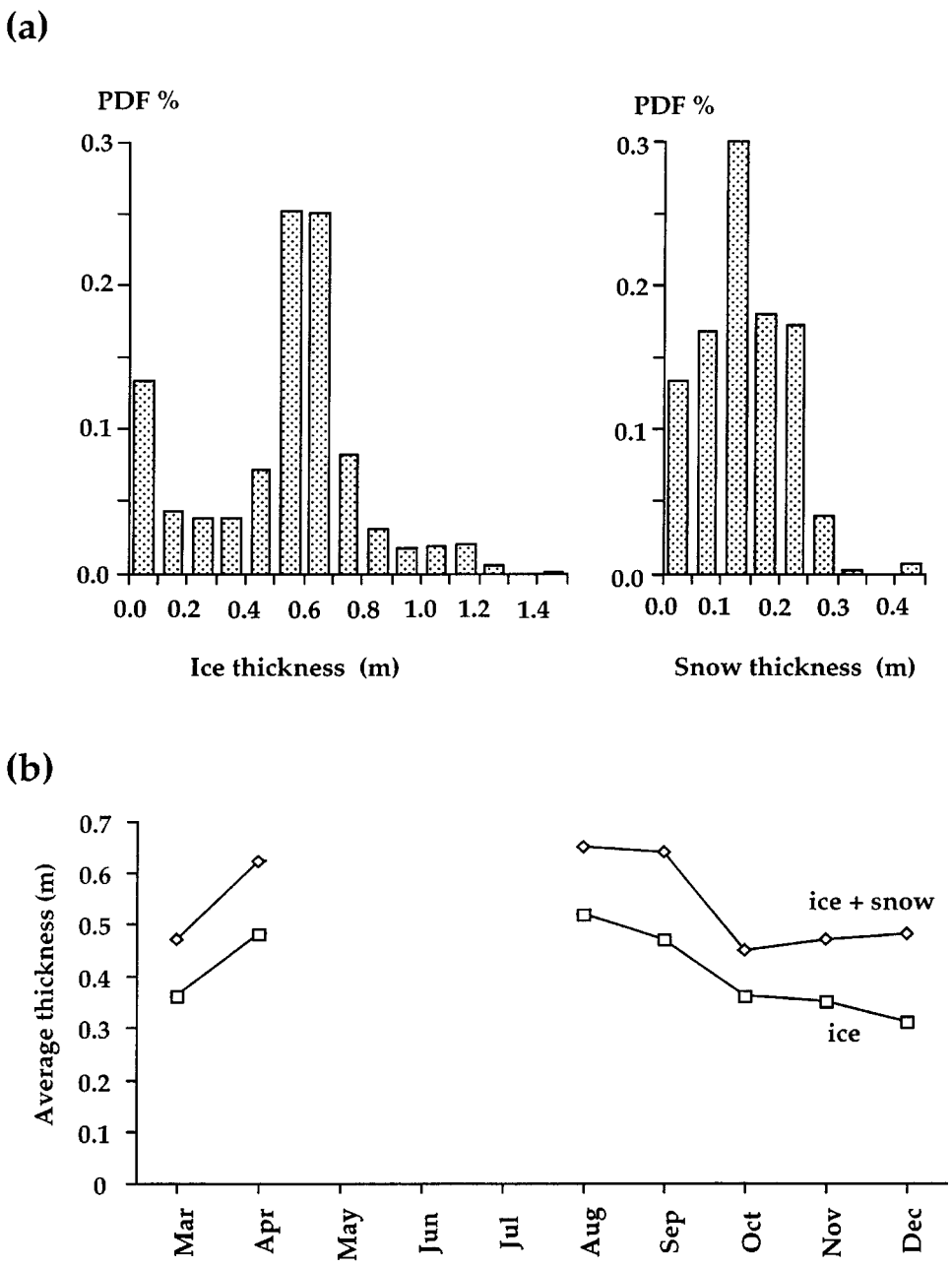

Fig. 3. Ice and snow thickness distributions for the east Antarctic sea ice zone derived from ship-based observations. (*a*) Typical thickness distributions of non-ridged ice, and of snow on that ice, at 140°E in August 1995. The lowest thickness category also includes open water areas. (*b*) The average non-ridged ice thickness, and snow thickness, averaged over the total ice extent between 60°E and 150°E as a function of time of year.

there is only a small fraction of the ice that is less than 0·4 m thick, since thin ice quickly thickens at this time of year. By October air temperatures and solar radiation are starting to increase, leads do not refreeze as quickly as in August, and thin ice thickens at a slower rate. As a result, there is more open water and a more uniform distribution across ice categories less than 0·7 m thick. The increased open water allows more solar radiation to be absorbed in the ocean providing a positive feedback and even further reducing new ice formation. By December continued surface warming has melted all thin ice, the open water fraction is over 50%, and mostly only ice greater than 0·6 m thick remains.

Fig. 3*b* shows the area-weighted average ice and snow thickness of non-ridged ice as a function of time of year. These averages include all observations in Fig. 2. The greatest average thickness of the non-ridged ice is probably less than 0·6 m, even in midwinter. Even though the individual floes are generally greater than 0·6 m thick in summer, the area-weighted average is considerably less because of the high open water fraction. The average thickness of snow on the ice remains relatively constant throughout the year, between 0·1 and 0·15 m. Note that with an average snow density of 350 kg m^{-3}, compared to an ice density of 900 kg m^{-3}, more than about 0·15 m of snow on 0·6 m thick ice will depress the surface below freeboard, and convert to 'snow-ice'.

The ice thickness estimates above apply only to the relatively thin and undeformed, non-ridged component of the pack. While rafting is the dominant dynamical mechanism by which floes reach 0·4–0·6 m thickness, continued convergence beyond that results in breaking and stacking of floes to form pressure ridges. The sail height (height above freeboard) of Antarctic ridges infrequently exceeds 1 m but measurements of surface profiles in the Antarctic (Lytle and Ackley 1992; Weeks *et al*. 1989) suggest that the ridged areas contain a disproportionately high fraction of the total ice mass within the pack. The distribution of thin ice and open water determines the exchange of heat, momentum and gas between the ocean and atmosphere, but the distribution of ridges strongly influences the total ice mass, and hence the mass of salt ejected to modify the underlying ocean.

Observations of ridged sea ice thickness are not easily obtained for the Antarctic where there are no sonar profiles available from military submarines, as in the Arctic. Drilled profiles across floes are only localised, but provide information on the small scale spatial variability in ice thickness. Allison and Worby (1994) used a number of such profiles to develop a simple model for calculating the effective mean thickness of ridged ice from ship-based observations of sail height and the extent of surface ridging. The total mean ice thickness estimated using this model with observations from seven voyages in the Indian Ocean sector varied from 1·5 to 3·2 times greater than the mean un-ridged ice thickness: the average factor over all voyages was 2·3 (Worby *et al*. 1997). Similarly, in the Bellingshausen Sea, Worby *et al*. (1996*b*) estimated a factor of 1·5 to 3. Ridges may be partially unconsolidated and contain some liquid sea water, and results from laser profiling studies suggest that the above corrected thickness values may overestimate the real mean thickness. Thus the ship-based observations provide an upper bound (ridging formulation) and lower bound (undeformed observations) for the total ice thickness, and hence ice volume, of the pack.

4. Ice Drift and Deformation

Pack ice is moved by winds and ocean currents and, compared with the ice cover in the central Arctic Basin, the Antarctic sea ice is highly mobile. Satellite-tracked data buoys, deployed either on ice floes or in the water between ice, have been used to investigate the ice drift and to collect surface meteorological data in the Weddell Sea, the Ross Sea, and around the coast of east Antarctica. In the Weddell Sea (e.g. Ackley 1982; Kottmeier *et al.* 1992) the ice drifts in a cyclonic gyre with 30-day mean drift speeds varying from $0{\cdot}05\,\mathrm{m\,s^{-1}}$ (4 km per day) in the south–west Weddell (75°S, 55°W) to almost $0{\cdot}2\,\mathrm{m\,s^{-1}}$ in the north–east Weddell (62°S, 10°W). The variance of this ice drift is high, generally ranging from $10^{-2}\,\mathrm{m^2\,s^{-2}}$ in the south–west, to $5{\times}10^{-2}\,\mathrm{m^2\,s^{-2}}$ in the north–east.

Australian ice drift studies have focussed on the east Antarctic region (Allison 1989; Worby *et al.* 1997) where the ice is generally less compact than in the Weddell Sea, and ice drift speeds are higher. Fig. 4 shows the trajectories of 30 buoys deployed in this region. The general pattern of drift is westward to the south of the Antarctic Divergence (variable in location, but typically at 63–65°S in the area shown), and eastward further north in the Antarctic Circumpolar Current. There are a number of areas such as Prydz Bay (75°E) and 90°E where there is net northward component to the drift, and overall the ice drift in the region is divergent, with most buoys eventually drifting north and out of the sea ice zone.

Measured mean daily drift speeds are as high as $0{\cdot}9\,\mathrm{m\,s^{-1}}$ (78 km per day), with an average for the whole region of $0{\cdot}22\,\mathrm{m\,s^{-1}}$. There is little difference in the average drift speed to the north or the south of the Antarctic Divergence, but there is some longitudinal variability. For example, mean westward drift rates in Prydz Bay ($0{\cdot}18\,\mathrm{m\,s^{-1}}$) and at 130°E ($0{\cdot}17\,\mathrm{m\,s^{-1}}$) are considerably less than around 40°E ($0{\cdot}34\,\mathrm{m\,s^{-1}}$). There is also an increase in average speed in the marginal ice zone, the outer 150–200 km of the pack where ice concentration is lower and floe sizes are smaller.

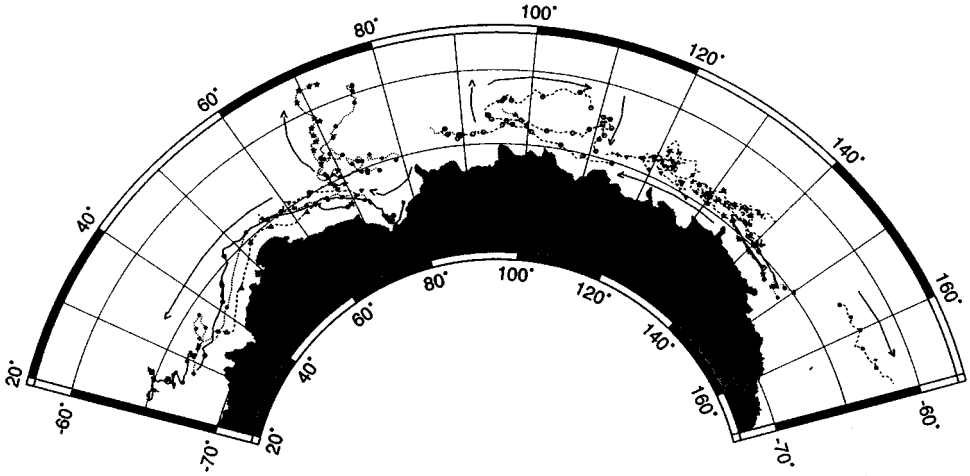

Fig. 4. Drift tracks of satellite-tracked data buoys deployed on ice floes in east Antarctica between 1985 and 1996. Symbols are plotted at the position of deployment, and at every subsequent 10 days. The direction of motion is generally westward south of 64–65°S, and eastward further north in the Antarctic Circumpolar Current.

The momentum balance describing sea ice drift includes terms for wind stress, water stress, Coriolis force, an internal stress between floes in contact, inertial forces, and ocean current effects. The wind stress is the most important force in determining the high day to day variability of the ice motion, particularly in the relatively low concentration ice of east Antarctica where the internal ice stress is small. Local changes in wind speed and direction, particularly those associated with the passage of synoptic storm systems, can accelerate the ice from near zero to more than $0{\cdot}8\,\mathrm{m\,s^{-1}}$ within hours (Worby *et al.* 1997). A power spectral density of Antarctic ice velocity typically shows a peak at a period of 4–7 days, similar to the peak in wind speed spectra due to synoptic systems. The strong correlation between ice motion and wind speed is shown in Fig. 5, a time series for August 1995 of wind speed at a height of 2 m above the surface and ice drift speed near 65·5°S, 140°E. The ice typically drifts at 2–3% of the wind speed, except during some periods of low wind speed with a northerly component, when the ice is under compression and internal stress terms are important (for example on days 218 and 230).

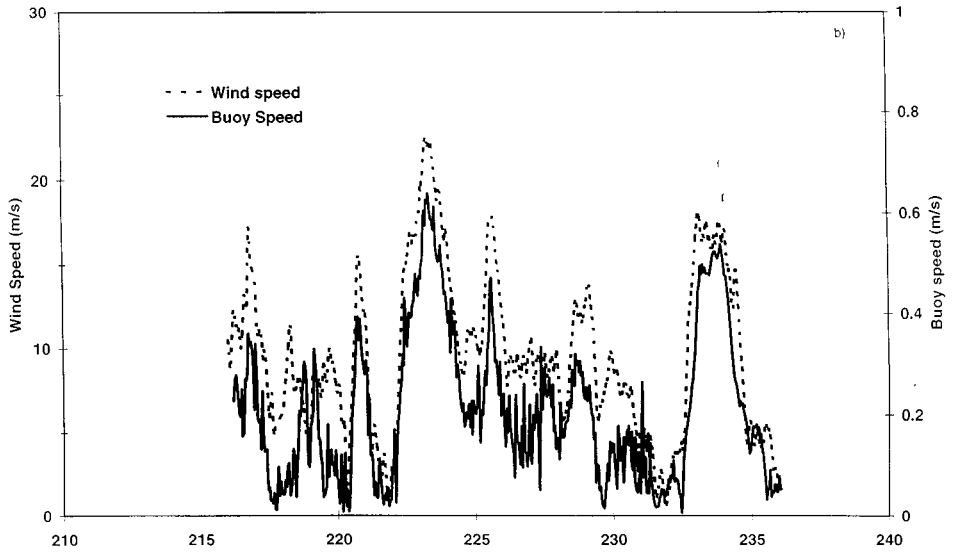

Fig. 5. Time series of wind speed (at 2 m above the surface) and ice drift speed (measured by satellite-tracked buoys) near 65·5°S, 140°E in August 1995.

Under free drift conditions the ice moves with a turning angle of 20–30° to the left of the wind direction (in the southern hemisphere). Hence, in the zone of westerlies to the north of the Antarctic divergence there is a component of average drift towards the unconstrained open ocean boundary to the north, and an average net divergence within the pack. This divergence is important in determining the location of the ice edge, and in creating new open water areas where rapid ice growth can occur. But differential motion between floes, due to the dependence of the wind drag on the surface roughness and ice thickness (Andreas *et al.* 1993), also causes local divergence and convergence, resulting

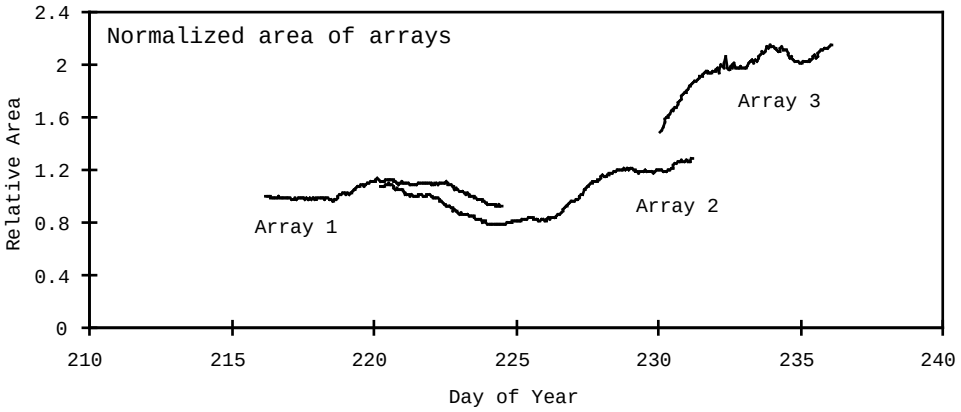

Fig. 6. Change in area within an ice field (about 40×40 km) measured by a composite array of ice buoys, for the same period as shown in Fig. 5. The area of each array is normalised by the original area of the first array. Arrays 2 and 3 are re-deployments of a subset of buoys from array 1, necessary to keep at least one array focussed on the study region. An expanding area indicates divergence, formation of open water areas, and new ice growth; a decreasing area indicates convergence and thickening of existing floes by rafting and ridge building.

in rafting of thinner ice, and creation of new leads. These dynamic processes control both the ice structure and the thickness distribution.

A winter-time experiment to investigate the role of drift and deformation on ice growth, and the resulting changes in the properties of Antarctic surface waters, was conducted from the Australian icebreaker *RSV Aurora Australis* in a 110×110 km region of the Antarctic pack ice near 64°S, 140°E during August 1995 (Worby *et al.* 1996*a*). The deformation of the pack was measured by an array of drifting buoys, spaced at distances between 1 to 45 km, and is summarised in Fig. 6. The first nine days of the experiment were characterised by one 'cycle' of divergence and convergence of the pack ice which resulted in significant increases in both the total ice mass and mean ice thickness within the pack. Divergence of the pack between days 218–220 increased the area of the array by 10–15% and subsequent convergence (days 221–225) decreased it again to an area smaller than the original array. There was a close relationship between wind direction and the expansion and compaction of the array. Expansion of the pack occurred during a period of south-westerly winds, when the ice had a net northerly drift away from the coast and when coincident low air temperatures caused leads to rapidly refreeze. Convergence occurred when the winds tended northerly or easterly, reversing the direction of ice drift toward the Antarctic continent and deforming much of the new ice by rafting and ridging. This period of convergence was accompanied by relatively high air temperatures, resulting in reduced ice growth at the base of existing floes, and possibly some melt on the thicker floes.

The second half of the experiment (days 225–236) was characterised by a prolonged period of pack ice expansion, during which time the area of the array more than doubled (Fig. 6). Despite this large divergence, the percentage of open water remained low (approximately 5%), as extreme temperatures as low as −30°C caused rapid freezing in the newly formed leads. The area of the array approximately doubled during the 21 day experiment, and net ice production,

which is the sum of growth at the base of existing floes plus new growth in leads, was estimated at between 0·31 and 0·49 m, averaged over the total area. Over the same period, there were very significant increases in the salinity of the ocean mixed layer, from a combination of salt rejection from the formation of sea ice and the possible entrainment of the saltier (and warmer) waters at the base of the mixed layer.

5. Concluding Remarks

In-situ data from a number of different regions of the Antarctic sea ice zone show that the ice characteristics and physical processes occurring there are very different from the better-known ice of the Central Arctic Basin. Many of the processes are sub-grid scale to climate models, and are not properly parametrised in most models at present. The dominant processes in the Antarctic sea ice zone are dynamic ones associated with the drift and deformation of the ice. Cycles of convergence and divergence, and of freezing, occur with the synoptic passage of storm systems around the Antarctic, and result in the alternate formation of thin new ice in leads, followed by thickening by deformation. Ice 0·5 to 0·6 m thick forms the basic 'building blocks' from which most thicker Antarctic pack is formed.

Acknowledgment

Much of the work reviewed in this paper has resulted from efforts of the sea ice group at the Antarctic CRC: the author acknowledges the contributions and enthusiasm of Tony Worby, Rob Massom, Vicky Lytle and Petra Heil.

References

Ackley, S. F. (1982). *In* 'Sea Level, Ice and Climate Change' (Ed. I. Allison), p. 177 (Int. Assoc. Hydrological Sciences: Oxford).
Allison, I. (1989). *GeoJournal* **18**, 103.
Allison, I., Brandt, R. E., and Warren, S. G. (1993). *J. Geophys. Res.* **98,** 12417.
Allison, I., and Worby, A. (1994). *Ann. Glaciol.* **20**, 195.
Andreas, E. L., Lange, M. A., Ackley, S. F., and Wadhams, P. (1993). *J. Geophys. Res.* **98**, 12439.
Gloersen, P., and Campbell, W. J. (1988). *J. Geophys. Res.* **93**, 10666.
Gloersen, P., Campbell, W. J., Cavalieri, D. J., Comiso, J. C., Parkinson, C. L., and Zwally, H. J. (1992). Arctic and Antarctic Sea Ice, 1978–87; Satellite Passive Microwave Observations and Analysis. NASA SP-511, Washington, DC, 290 pp.
Gow, A. J., Ackley, S. F., Weeks, W. F., and Govoni, J. W. (1982). *Ann. Glaciol.* **3**, 113.
Heil, P., Allison,I., and Lytle, V. (1996). *J. Geophys. Res.* **101**, 25741.
Jacka, T. H., Allison, I., Thwaites, R., and Wilson, J. C. (1987). *Ann. Glaciol.* **9**, 85.
Jeffries, M. O., and Weeks, W. F. (1993). *Antarctic Science* **5**, 63.
Jeffries, M. O., Worby, A. P., Morris, K, and Weeks, W. F. (1996). *J. Glaciol.* **43**, 138.
Johannessen, O. M., Miles, M., and Bjorgo, G. (1995). *Nature* **376**, 126.
Kottmeier, C., Olf, J., Frieden, W., and Roth, R. (1992). *J. Geophys. Res.* **97**, 20373.
Lange, M. A. (1988). *Ann. Glaciol.* **10**, 95.
Lange, M. A., Ackley, S. F., Wadhams, P., Dieckmann, G. S., and Eicken, H. (1989). *Ann. Glaciol.* **12**, 92.
Lange, M. A., and Eicken, H. (1991). *J. Geophys. Res.* **96**, 4821.
Lytle, V. I., and Ackley, S. F. (1992). *Ant. J. U.S.* **27**, 93–4.
Wadhams, P., Lange, M. A., and Ackley, S. F. (1987). *J. Geophys. Res.* **92**, 14535.
Weeks, W. F., Ackley, S. F., and Govoni, J. W. (1989). *J. Geophys. Res.* **94**, 4984.
White, W. B., and Peterson, R. G. (1996). *Nature* **380**, 699.

Worby, A. P., Bindoff, N. L., Lytle, V. I., Allison, I., and Massom, R. A. (1996*a*). *EOS* **77**, 453.
Worby, A. P., Jeffries, M. O., Weeks, W. F., Morris, K., and Jana, R. (1996*b*). *J. Geophys. Res.* **101**, 28441.
Worby, A. P., Masssom, R. A., Allison, I., Lytle, V. I., and Heil, P. (1997). East Antarctic sea ice: a review of its structure, properties and drift. *AGU Ant. Res. Series* (in press).
Zwally, H. J., Comiso, J. C., Parkinson, C. L., Campbell, W. J., Carsey, F. D., and Gloersen, P. (1983). Antarctic Sea Ice, 1973–6: Satellite passive microwave observations. NASA SP-459, Washington, DC, 206 pp.

Manuscript received 12 November 1996, accepted 23 May 1997